

Thermal stabilization of polyacrylonitrile fibres

Stephen Dalton, Frank Heatley, Peter M. Budd*

Department of Chemistry, University of Manchester, Manchester M13 9PL, UK

Received 24 August 1998; received in revised form 26 October 1998; accepted 26 October 1998

Abstract

A polyacrylonitrile (PAN) fibre, Dralon T (DT), and a copolymer manufactured as a carbon fibre precursor, Special Acrylic Fibre (SAF), were studied as received and after heat-treatment in air at various temperatures up to 300°C. Wide angle X-ray scattering (WAXS) was undertaken on single fibres, fibre bundles and films, utilizing both conventional and synchrotron sources. With a conventional source, the normal WAXS pattern was observed for both polymers, i.e. two main equatorial reflections, a diffuse equatorial reflection and a diffuse off-equatorial reflection. With a synchrotron source, seven equatorial WAXS reflections could be detected in DT. Also, a sharp, meridional reflection was observed in SAF as received and in DT after stretching at 100°C. Unpolarized and polarized infra-red spectra were obtained from single fibres and films by FTIR microscopy. A measure of the extent of reaction (EOR) following heat-treatment was derived from the intensity of the nitrile absorption and the intensity of absorption at 1600 cm⁻¹: $EOR = [I_{1600}/(I_{CN} + I_{1600})]$. Two complementary measures of orientation were used to follow changes on heat-treatment: the peak width at half-height of an azimuthal plot of the most intense WAXS reflection and the nitrile dichroic ratio from FTIR microscopy. For fibres held under tension during heat-treatment, the degree of orientation by either measure did not decrease until the EOR exceeded 0.5. Solid-state ¹³C NMR, together with IR results, indicated that at least three chemical processes occurred on heat-treatment: nitrile reaction, conjugated C = C formation and oxidation. © 1999 Elsevier Science Ltd. All rights reserved.

Keywords: Polyacrylonitrile; Carbon fibre; Wide angle X-ray scattering

1. Introduction

Fibres of polyacrylonitrile (PAN), usually including a comonomer, find application in textiles and as carbon fibre precursors [1]. For carbon fibre production, PAN fibres are stabilized by heating in air at temperatures in the range 200°C–300°C, prior to carbonization in an inert atmosphere at temperatures above 1000°C [2].

Various reaction schemes have been proposed to occur during stabilization, as reviewed by Bashir [3]. Houtz [4] suggested the formation of a heteroaromatic, cyclic structure (Table 1, structure **a**). Later workers [5–8] have favoured a cyclic polyimine structure frequently referred to as ‘‘ladder polymer’’ (Table 1, structure **b**), which may undergo tautomerization to a polyenamine (Table 1, structure **c**), followed by isomerization and further reaction [9–11]. It has also been suggested that various types of intermolecular crosslinking may arise [12–14] (Table 1, structures **d–f**) or that dehydrogenation may result in conjugated polyenes (Table 1, structure **g**) [15,16]. On stabilization in

air, oxygen is incorporated into the fibre and reactions leading to nitrone [17], ketone [18], epoxide [18], lactone [19], lactam [19] and other structures [20] have been suggested. Ferguson and Mahapatro [21] proposed that oxidative chain degradation competes with cyclisation. Jellinek and Das [22] attributed the production of HCN on thermal oxidative degradation at temperatures above 250°C to a process involving chain scission.

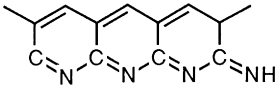
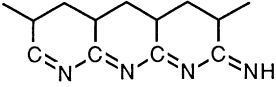
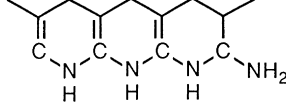
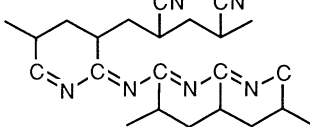
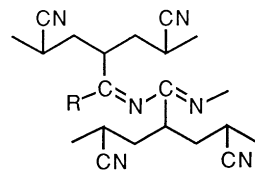
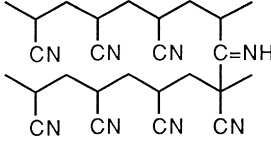
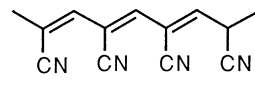
It is generally thought that the better the degree of molecular orientation in the original PAN fibre, the better the mechanical properties, in particular the modulus, of the resultant carbon fibre [23,24]. However, despite more than 40 y of research, there is still much uncertainty regarding the nature of the molecular order in PAN and the microstructural and chemical changes which take place during stabilization.

Wide angle X-ray scattering (WAXS) of drawn PAN fibres shows two strong equatorial reflections (Bragg spacings $d \approx 3.0 \text{ \AA}$ and $d \approx 5.3 \text{ \AA}$), indicating order perpendicular to the fibre axis, but off-equatorial reflections are generally diffuse. These results have frequently been interpreted in terms of hexagonal packing of ‘‘molecular rods’’ comprising distorted helices [13,25,26] or kinked planar zig-zags [27]. Some have assumed a single, laterally ordered

* Corresponding author. Tel.: 0044 0161 275 4706; fax: 0044 0161 275 4598.

E-mail address: Peter.Budd@man.ac.uk (P.M. Budd)

Table 1
Possible structures which may arise in stabilised PAN

	Structure	Reference
a	Heteroaromatic cyclic structure 	Houtz [4]
b	Polyimine cyclic structure (ladder polymer) 	Grassie et al. [5,6] Burlant and Parsons [7] LaCombe [8]
c	Polyenamine cyclic structure 	Coleman and Petcavich [9] Fochler et al. [10] Xue et al. [11]
d	Propagation crosslink 	Grassie and Hay [12]
e	Intermolecular nitrile crosslink 	Olivé and Olivé [13]
f	Azomethine crosslink 	Schurz [14]
g	Conjugated polyene 	Berline et. al. [15] Fester [16]

[28–34] or paracrystalline [35] phase, whilst others propose a two-phase structure with regions of ordered rods and regions of amorphous material [36–40] or disordered rods [41,42].

Under certain conditions, the main equatorial reflections from PAN appear to be doublets [43,44] and additional peaks have been observed, leading some workers to assign three-dimensional, orthorhombic unit cells [44–47]. Diffuse scattering at $d \approx 3.3 \text{ \AA}$ has been referred to as an “amorphous halo” and, on this basis, degrees of crystallinity of 30% or more have been reported [48,49]. Commercial PAN is essentially atactic. If it is regarded as a conventional

semi-crystalline polymer, such high degrees of crystallinity require either two separate crystalline phases, one of syndiotactic sequences and one of isotactic sequences [44], or a mixed tacticity phase, incorporating “shape emulating” conformations [50,51]. Alternatively, if PAN is regarded as having a single-phase structure, the scattering at $d \approx 3.3 \text{ \AA}$ may arise from rotational disorder of molecular rods [27].

There have been a number of previous studies of the changes in microstructure which occur on heat-treatment of PAN fibres, utilizing such techniques as WAXS [39,41,52–59], small angle X-ray scattering [39,58–61]

and infra-red spectroscopy [57,58]. The arc width of the strongest equatorial reflection in the WAXS pattern provides an indication of the degree of orientation [56,62]. When carrying out WAXS studies of PAN fibres using a conventional source, it has been necessary to use a bundle of fibrils in order to obtain adequate scattering intensity. For quantitative studies of orientation, non-parallel alignment of fibrils in a bundle is likely to introduce a systematic error into the results. In the present work, a synchrotron source enabled single fibres to be studied and a comparison made with bundle data. Fourier Transform Infrared (FTIR) microscopy was also employed in studies of single fibres, to obtain information about chemical changes and, using polarized radiation, about molecular orientation. ^{13}C NMR was used to obtain further information about the chemical changes occurring on stabilization.

The aims of this study were (i) to evaluate techniques for the study of single fibres and (ii) to investigate the chemical and microstructural changes occurring on stabilization in air. Two commercial fibres were used, a homopolymer PAN, ‘‘Dralon T’’ (DT), and a copolymer manufactured as a carbon fibre precursor, ‘‘Special Acrylic Fibre’’ (SAF). The fibres were studied as received and after heat-treatment in air for various times at temperatures in the range 200°C–300°C. Heat-treatments were carried out both with the samples maintained under tension, as they are during carbon fibre production, and with the fibres allowed to relax. Some experiments were also undertaken on fibres annealed and stretched at 100°C, and on films prepared from DT and SAF.

2. Experimental

2.1. Fibres

The homopolymer PAN fibre, DT, was supplied by Bayer on a reel as a continuous twisted tow. Fibres were manually untwisted before experiments were carried out. The diameter of a DT fibril was estimated from microscopy as 15–20 μm .

The copolymer fibre, SAF, was supplied by Courtaulds on a reel in a continuous, untwisted form, with each tow consisting of 6000 fibrils. The diameter of a SAF fibril was estimated from microscopy as 8–12 μm . The composition of SAF is reported [63] as 93% acrylonitrile, 6% methyl acrylate and 1% itaconic acid. SAF was manufactured as a precursor for carbon fibre production.

2.2. Stabilization of fibres

Stabilization of fibres was carried out in a Carbolite furnace with a Eurotherm temperature controller. Two samples were treated simultaneously, each clamped at one end to a brass holder. One sample was held under tension by applying a 360 g weight. The second sample was allowed to relax during heat-treatment. The mass of sample was about

0.2 g in each case. Heat-treatments were carried out at temperatures of 200°C, 225°C, 250°C, 275°C and 300°C for various times between 5 and 90 min, and at 100°C for 16 h. In addition, an experiment was undertaken in which fibres were stretched at 100°C, over a 2 h period, by about 30% of their original length.

For solid-state ^{13}C NMR, at least 600 mg of sample was required, so bundles of five tows of SAF (approximate weight 1 g), and similar amounts of DT, were used to carry out stabilization at 225°C. Samples were held under tension, as otherwise such large samples fused during heating and underwent large weight loss.

2.3. Films

Films were prepared from DT and SAF as follows: A solution of the polymer (3% by weight in dimethylformamide) was poured into a crystallising dish then placed in an oven at 80°C for 48 h. The resulting film was washed twice with distilled water for 24 h and dried under vacuum for 48 h. To induce orientation, samples of DT film were slowly stretched by 100% at a temperature of 150°C and samples of SAF film were stretched by 100% and 200% at 110°C. Films of DT were more brittle than those of SAF, and could not be stretched to the same extent.

2.4. Elemental analysis

Elemental analysis was carried out by the Department of Chemistry Microanalysis Service, University of Manchester. Both fibres were analysed for C, H, N and, in the light of a report in the literature [64], for traces of Ca, K, Na and Mg.

2.5. ^{13}C nuclear magnetic resonance spectroscopy

High resolution ^{13}C NMR spectra were obtained for solutions of DT and SAF [20% by weight in deuterated dimethylsulphoxide(DMSO- d_6)] at ambient temperature in 10 mm o.d. NMR tubes using a Varian Associates Unity 500 Spectrometer operating at 125 MHz, with a flip angle of 60° and a recycle time of 10 s. Solution spectra were also obtained for material extracted with DMSO- d_6 from stabilized fibre samples.

Cross-Polarization/Magic Angle Spinning (CP/MAS) ^{13}C NMR was carried out using a Varian Unity 300 spectrometer operating at 75.5 MHz, equipped with a Doty Scientific Industries Inc. 7 mm CP/MAS probe. Approximately 600 mg of chopped fibre were packed into a ZrO₂ rotor with Kel-F caps. Spectra were obtained with a contact time of 2 ms and a recycle time of 5 s. The ^1H decoupling field was 45 kHz.

2.6. Fourier transform infra-red microscopy

FTIR microscopy was carried out on single fibres, mounted under slight tension with double-sided sticky tape, using a Spectra-Tech IR Plan microscope attached to

Table 2
Results of elemental analysis for DT and SAF fibres (calculated figures in parentheses)

Element	DT	SAF
C	67.95% (67.9)	67.4% (66.9)
H	5.85% (5.7)	5.4% (5.8)
N	25.3% (26.4)	23.5% (24.6)
Ca	158.0 ppm	136.4 ppm
K	0	0
Na	281.3 ppm	1802.6 ppm
Mg	13.9 ppm	24.7 ppm

a Digilab FTS-40 spectrometer. Spectra were recorded over a spectral range of 4000–800 cm^{-1} , with 256 scans typically being collected, using a liquid nitrogen cooled mercury–cadmium–telluride detector. A gold-wire grid polarizer was used for orientation studies. When using the polarizer, spectra were acquired with the polarizer set both parallel and perpendicular for the same region of fibre.

As an indication of orientation, dichroic ratios D were calculated for the nitrile absorption and, in the case of

SAF, the CO absorption, using $D = [(A_{\parallel} - A_{\perp}) / (A_{\parallel} + A_{\perp})]$, where A_{\parallel} is the absorption with the electric vector of polarized IR radiation parallel to the fibre axis and A_{\perp} is the absorption with the electric vector of polarized IR radiation perpendicular to the fibre axis. Values of D range in principle from -1 for perfect orientation of the transition moment perpendicular to the fibre axis to $+1$ for parallel orientation of the transition moment. From repeat experiments, confidence limits in values of D were ± 0.02 . It should be noted that other workers have expressed dichroic ratio in a variety of different ways [A_{\parallel}/A_{\perp} , A_{\perp}/A_{\parallel} or $(A_{\parallel} + A_{\perp}) / (A_{\parallel} - A_{\perp})$] [65,66]. Various models of orientation may be applied to polymers in order to obtain orientation parameters and for PAN it has been shown that, if the Kratky orientation model is applicable, the transition moment for the nitrile group is at an average angle of about 70° to the chain axis [67]. Bashir et al. [66] have argued on empirical evidence that an angle of 73° is more realistic and they used this value in calculations of orientation factors for uniaxially drawn PAN films from IR dichroism. In the present work, values of D were used simply to follow changes in orientation and no attempt was made to calculate orientation factors.

2.7. Wide angle X-ray scattering

WAXS was carried out using both a conventional source and a synchrotron source. Conventional studies of fibre bundles utilized a Philips generator (CuK α radiation, wavelength $\lambda = 1.5418 \text{ \AA}$) with a 1 mm diameter collimator and a flat plate camera. Synchrotron studies, both of fibre bundles and of single fibres, utilized Station 7.2 of the Synchrotron Radiation Source (SRS) at the Daresbury Laboratory, where a bent triangular Ge (1 1 1) monochromator provides a monochromatic X-ray beam ($\lambda = 1.488 \text{ \AA}$, $\Delta\lambda/\lambda = 0.0004$). Samples were mounted on lead discs with a 2 mm diameter hole, and held in an evacuated (30–60 mmHg) chamber. For experiments in which orientation measurements were to be made, the samples were brushed with calcite to provide well-defined diffraction rings to aid analysis. A flat plate camera was used with a nominal sample to film distance of 60 mm. Collimators used were typically 0.2 mm diameter when studying a fibre bundle and 0.8 mm for single fibre samples.

Interplanar spacings d were calculated using the Bragg equation, $n\lambda = 2d \sin \theta$, where n is the order of reflection and for the flat plate camera the Bragg angle θ is calculated using the relationship $\tan 2\theta = r/D$, where r is the measured radius of a diffraction peak and D is the sample-to-film distance. It should be noted that use of the Bragg equation is not necessarily the most appropriate way to treat a poorly ordered polymer [68], nevertheless d spacings calculated in this way provide a useful basis for comparison with the literature.

For orientation studies, WAXS photographs were digitised with a Joyce-Loebl Scandig 3 microdensitometer and

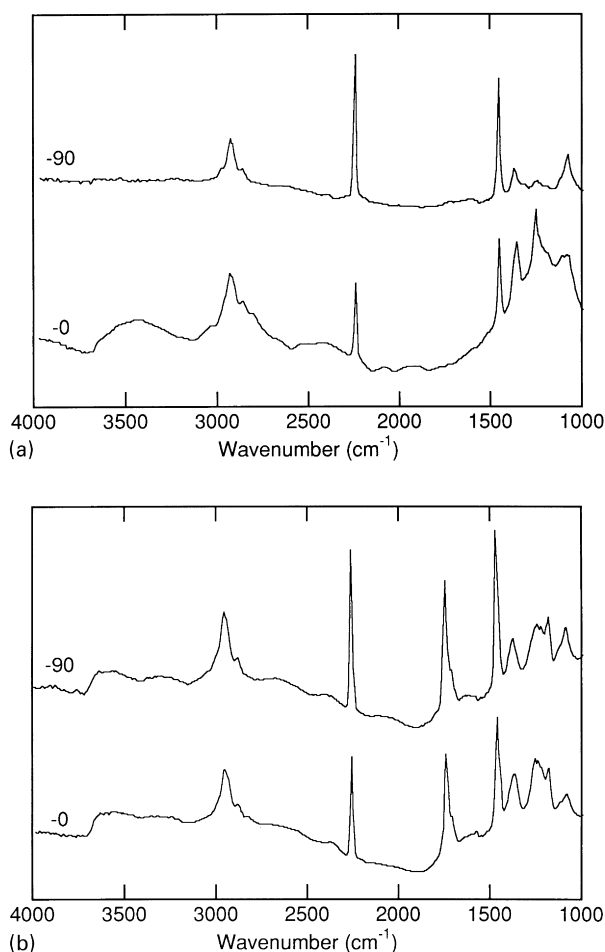


Fig. 1. Polarized infra-red spectra from single fibres of (a) DT and (b) SAF, with electric vector parallel (–0) and perpendicular (–90) to the fibre axis.

Table 3
Triad abundances

Tacticity	Triad	DT		SAF	
		Exp.	Calc. $P_m = 0.46$	Exp.	Calc. $P_m = 0.49$
Isotactic	mm	0.235	0.21	0.21	0.24
Heterotactic	mr	0.48	0.50	0.52	0.50
Syndiotactic	rr	0.285	0.29	0.27	0.26

azimuthal plots were obtained using a routine adapted from the Daresbury GENS suite of programs. The peak width at half height for an azimuthal plot of the reflection at $d = 5.3 \text{ \AA}$ was taken as a measure of the degree of orientation within the fibre of the scattering planes. Increased orientation is reflected in a smaller value of azimuthal peak width. From repeat experiments, confidence limits in values of azimuthal peak width were $\pm 1.2^\circ$.

3. Results

3.1. Composition of Dralon T and special acrylic fibre

The results of elemental analysis are given in Table 2. Polarized FTIR spectra obtained from single fibres of DT and SAF are shown in Fig. 1. The baseline could have been improved by flattening the fibres, but this was not done in the present work as it would have affected the microstructure. Spectra for both fibres showed prominent peaks at 2940 cm^{-1} (CH stretch), 2240 cm^{-1} (CN stretch) and 1452 cm^{-1} (CH₂ bend). For SAF the carbonyl stretch of comonomer units appeared at 1730 cm^{-1} .

¹³C NMR spectra for both types of fibre showed the three main resonances of the acrylonitrile unit (CH: 27 ppm; CH₂: 33 ppm; CN: 120 ppm). For SAF, peaks attributable to methyl acrylate comonomer were visible (CH: 41 ppm; OCH₃: 52 ppm; CO: 174 ppm).

3.2. Stereochemistry of Dralon T and special acrylic fibre

The CH carbon of the acrylonitrile repeat unit gave rise to three well resolved peaks in ¹³C NMR spectra, which were used to determine triad tacticity. Assignments of these peaks were originally made by Shaefer [69] and confirmed by Turska [70]. Triad abundances are given in Table 3, where m stands for meso (same configuration) and r for racemic (opposite configuration) addition of the monomer to the growing chain end. The results were analysed using Bovey's [71] procedure and a Bernoullian model was found to apply within experimental error, the probability of meso addition P_m being 0.46 for DT and 0.49 for SAF. Triad probabilities calculated using these values of P_m are included in Table 3. The results show that both polymers were essentially atactic.

3.3. Bragg spacings

X-ray photographs of fibre bundles taken using a conventional source showed, for both fibres, two main equatorial peaks ($d \approx 3.0 \text{ \AA}$ and $d \approx 5.3 \text{ \AA}$), a third diffuse equatorial peak ($d \approx 3.3 \text{ \AA}$), a diffuse meridional peak ($d \approx 2.3 \text{ \AA}$) and a diffuse off-equatorial peak ($d \approx 3.5 \text{ \AA}$), as has been reported previously for PAN fibres [13,25–42].

X-ray photographs taken using a synchrotron source provided additional detail. For the homopolymer fibre DT, photographs of fibre bundles (Fig. 2(a)) showed two

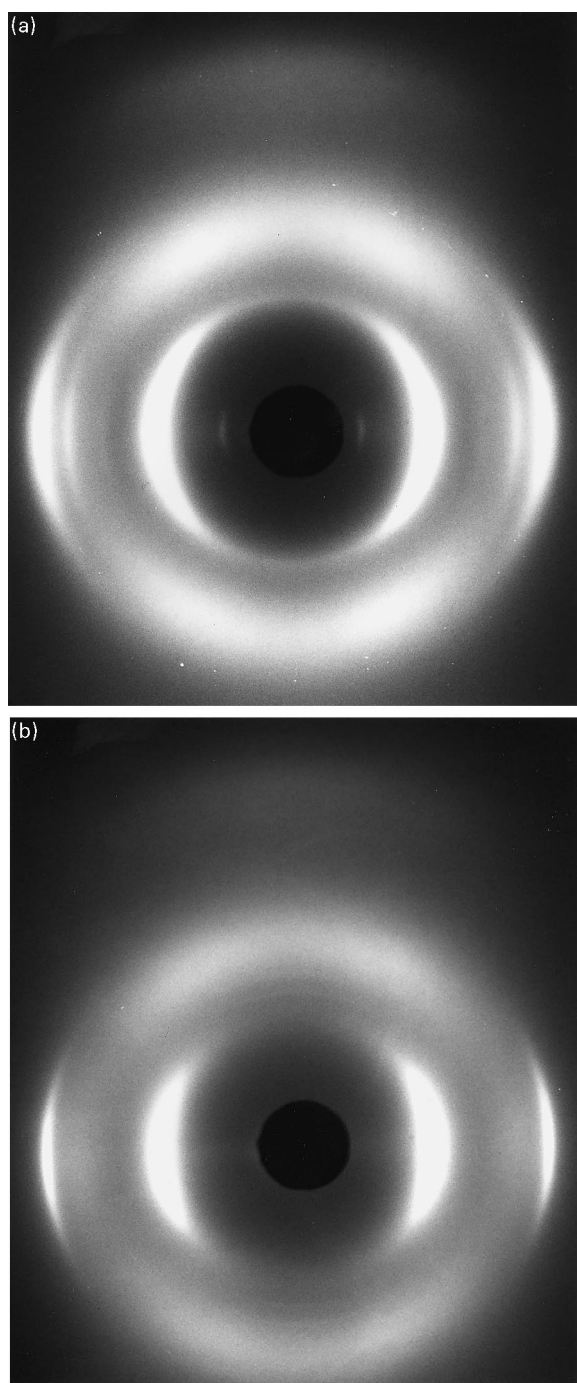


Fig. 2. Synchrotron WAXS from bundles of (a) pristine DT and (b) SAF heat-treated for 45 min at 200°C .

Table 4
Equatorial Bragg spacings for PAN: experimental results and values calculated for cell of Klement and Geil [31]

Sample	Reference	$d(\text{\AA})$					
DT fibre	This work	2.93, 3.01	3.34	3.85	5.11, 5.25	10.00	
SAF fibre	This work	3.05	3.3		5.29		
Fibre	Stéfani et al [44,45]	1.95, 2.54, 2.64	3.0		5.1, 5.26		
Fibre/DMF	Walner and Riggert [30]	2.44, 2.60, 2.71	3.05	3.35	3.56, 3.84, 4.16, 4.52	5.18	5.73
Fibre	Colvin and Storr [46]	2.4, 2.6	3.1		5.4		
Film/H ₂ O	Bashir et al [33]	2.90, 3.04	3.33		5.11, 5.31	10.10	
Crystal	Holland et al. [43]	2.6	2.9, 3.0		5.1, 5.3		
Crystal	Klement and Geil [31]	2.53, 2.65	2.90, 3.02	3.64, 3.91	5.05, 5.36	7.81	10.07
Calculated d			2.90, 3.02	3.37	3.91	5.09, 5.30	10.18
hkl			0 4 0, 6 2 0	6 1 0	4 2 0	2 2 0, 4 0 0	1 1 0

Table 5
Off-equatorial Bragg spacings for PAN

Sample	Reference	$d(\text{\AA})$			
DT fibre	This work	~ 2.3	3.5		
SAF fibre	This work	~ 2.3	3.5	4.15	
Fibre	Stéfani et al. [44,45]	2.28	3.6		
Fibre	Colvin and Storr [46]	1.8	2.8	3.5	4.0

additional equatorial peaks ($d = 3.85 \text{ \AA}$ and $d = 10.0 \text{ \AA}$), and photographs of single fibres indicated that the main equatorial peaks were doublets. The equatorial Bragg spacings may be indexed in terms of the unit cell of Klement and Geil [31] as $hk0$ reflections for an orthorhombic structure with $a = 21.18 \text{ \AA}$ and $b = 11.60 \text{ \AA}$ (Table 4).

For the copolymer fibre SAF, photographs of fibre bundles showed the normal pattern together with an

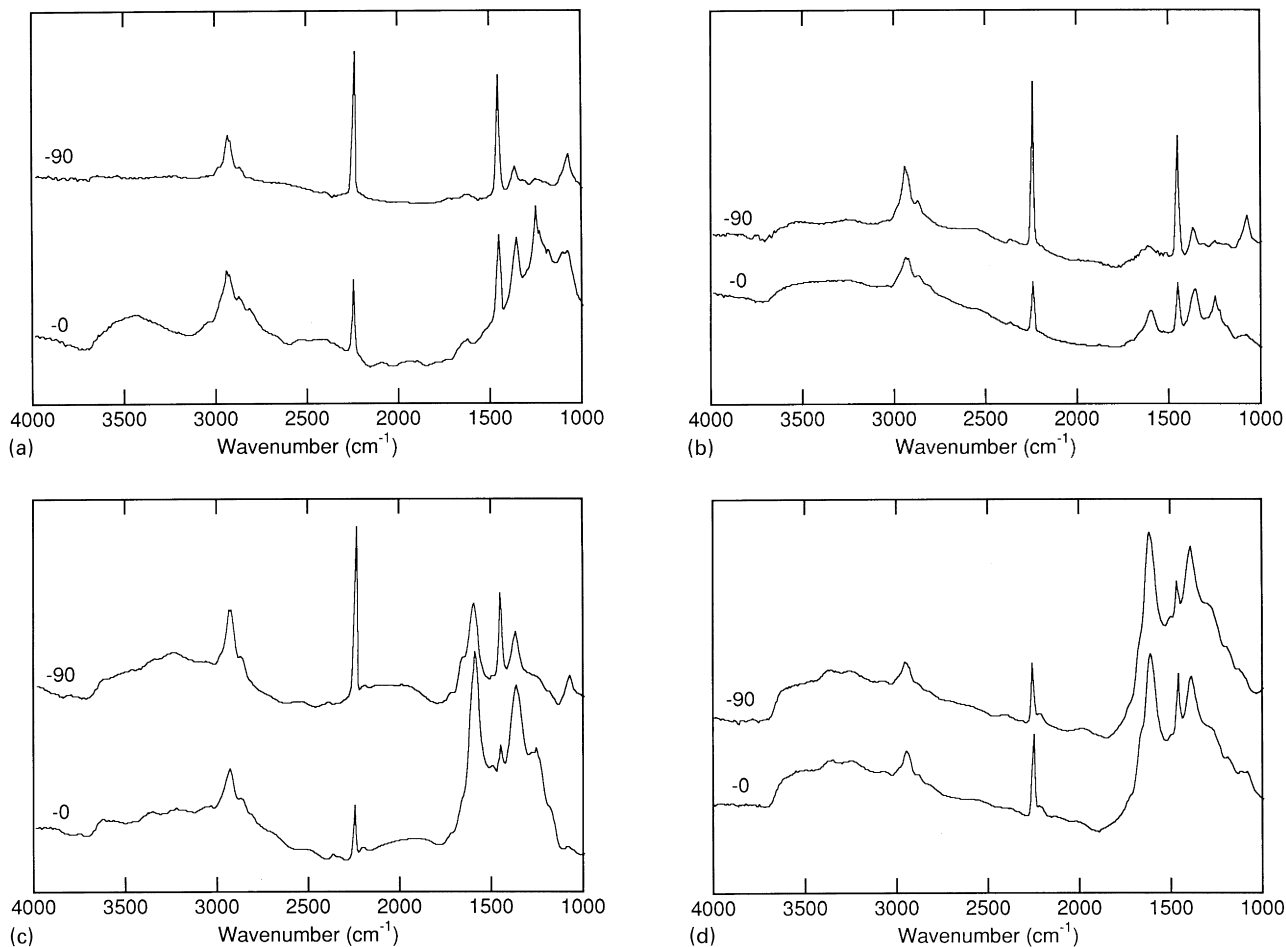


Fig. 3. Polarized infra-red spectra from single fibres of DT after heat-treatment for 15 min. at (a) 225°C, (b) 250°C, (c) 275°C and (d) 300°C, with electric vector parallel (– 0) and perpendicular (– 90) to the fibre axis.

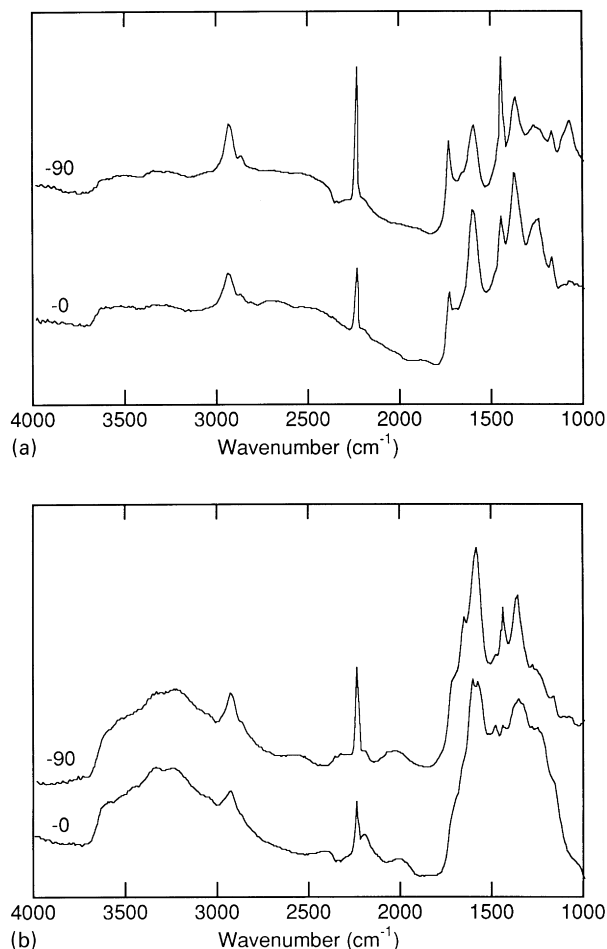


Fig. 4. Polarized infra-red spectra from single fibres of SAF after heat-treatment at 225°C for (a) 15 min. and (b) 45 min, with electric vector parallel (– 0) and perpendicular (– 90) to the fibre axis.

additional, sharp meridional peak ($d = 4.15 \text{ \AA}$). On heat-treating SAF for 45 min at 200°C under tension, a second sharp, meridional peak ($d = 4.59 \text{ \AA}$) appeared (Fig. 2(b)). The second meridional peak disappeared after 60 min and the original peak was extremely faint after 90 min at 200°C. No such peak was seen for DT fibre as received, but after stretching at 100°C a sharp meridional peak ($d = 4.18 \text{ \AA}$) appeared.

The observed d spacings from synchrotron WAXS for the pristine fibres are summarised in Tables 4 and 5, together with comparative data from the literature. X-ray scattering from cast films of DT and SAF exhibited two very broad, diffuse halos ($d \approx 3.0 \text{ \AA}$ and $d \approx 5.3 \text{ \AA}$), which became equatorial arcs on stretching.

On stabilization, the intensities of the WAXS peaks attributable to PAN decreased, and an equatorial peak appeared at $d \approx 3.6 \text{ \AA}$, which has been attributed to the formation of ‘‘ladder polymer’’ [56].

3.4. Chemical changes on stabilization

Examples of single-fibre polarised FTIR spectra, with

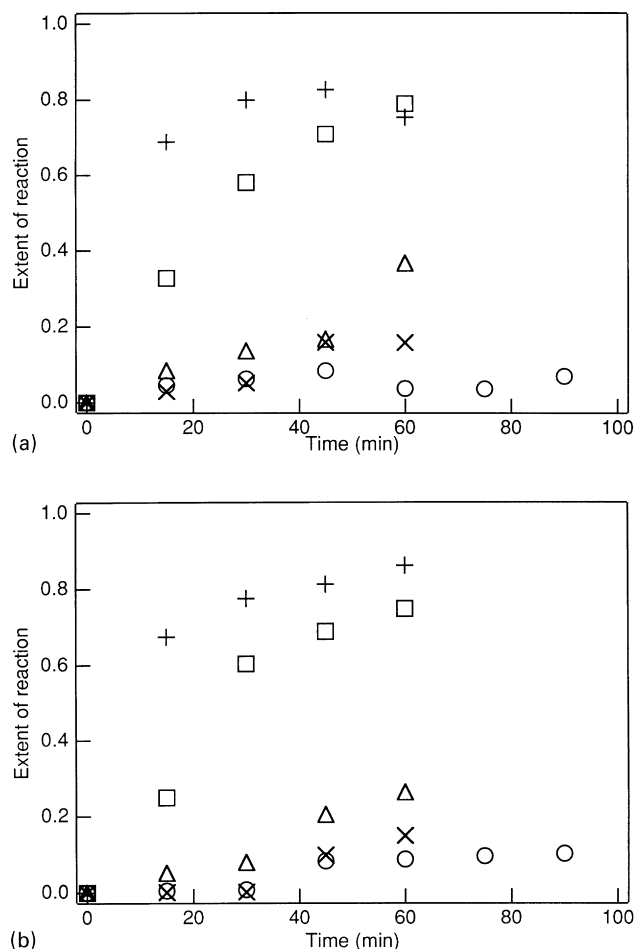


Fig. 5. Dependence on time of extent of reaction for DT heat-treated (a) under tension and (b) without tension, at (O) 200°C, (X) 225°C, (Δ) 250°C, (□) 275°C and (+) 300°C.

electric vector parallel (– 0) and perpendicular (– 90) to the fibre axis, are shown in Figs. 3 and 4. Fig. 3 shows spectra of DT after heat treatment for 15 min. at various temperatures and Fig. 4 shows spectra of SAF after heat-treatment at 225°C for two different times. Important changes observed on stabilization were as follows:

1. The nitrile absorption (2240 cm^{-1}) decreased in intensity.
2. A broad peak at 1600 cm^{-1} appeared and grew. This peak was generally more intense in the – 0 spectrum than in the – 90 spectrum, and it split into two peaks (1620 and 1580 cm^{-1}) at longer times and higher temperatures. Peaks in this region have variously been assigned to conjugated C=C [17,19] or to $(\text{C}=\text{N})_n$ structures [6], or to a combination of the two [10,72]. The observation of two peaks in – 0 spectra suggests a combination.
3. A peak appeared at 2200 cm^{-1} . This may be attributed to a conjugated nitrile group, which could arise from dehydrogenation [10,73], or from tautomerization and isomerisation of ‘‘ladder’’ polymer [9–11].

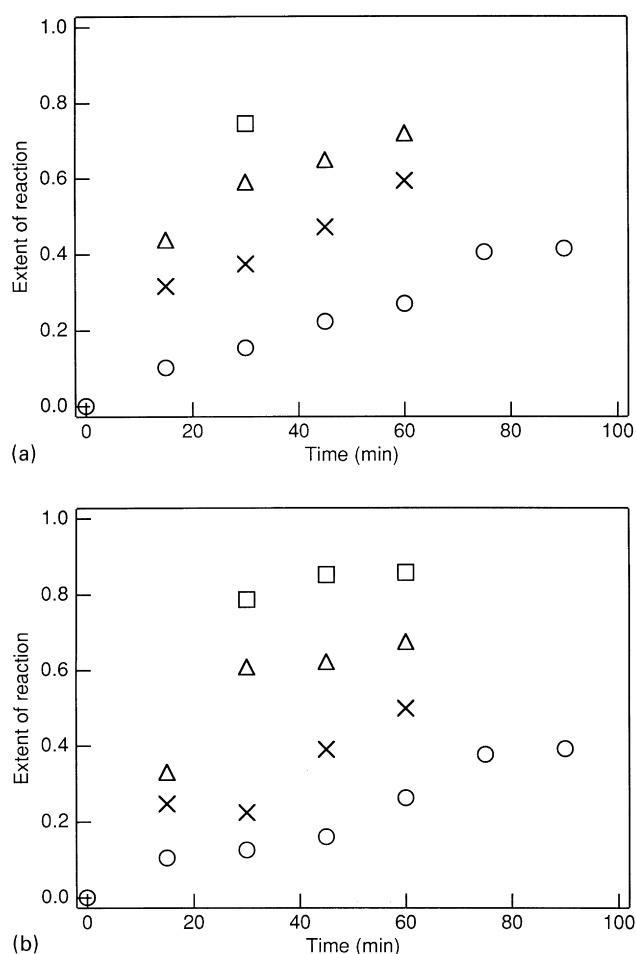


Fig. 6. Dependence on time of extent of reaction for SAF heat-treated (a) under tension and (b) without tension, at (○) 200°C, (×) 225°C, (Δ) 250°C and (□) 275°C.

- A peak appeared at 1680 cm^{-1} as a shoulder on the broad peak at 1600 cm^{-1} . This may be attributed to carbonyl formed on oxidation [10,74].
- For SAF, the comonomer carbonyl peak at 1730 cm^{-1} decreased.

The intensity of the peak at 1600 cm^{-1} , I_{1600} , and the intensity of the nitrile peak at 2240 cm^{-1} , I_{CN} , were used to provide for comparative purposes an internal indication of extent of reaction, $\text{EOR} = [I_{1600}/(I_{\text{CN}} + I_{1600})]$ [75]. The value of EOR varies from 0 for no reaction to 1 for complete

reaction of nitrile groups. Values of EOR are shown as a function of time in Figs. 5 and 6 for DT and SAF, respectively, at various temperatures.

Fig. 7 compares the solid state ^{13}C CP/MAS NMR spectra for SAF heat-treated at 225°C for 15 min (Fig. 7(b)) and for 60 min (Fig. 7(c)) with that of the untreated fibre (Fig. 7(a)). The spectrum for the untreated fibre was obtained using the TOSS (Total Suppression of Sidebands) technique [76], but the spectra of the heat-treated samples were obtained without TOSS. Residual chemical shielding anisotropy spinning sidebands (TOSS) and actual sidebands (no TOSS) are indicated. All spectra show peaks at 30 ppm (backbone CH + CH₂), 120 ppm (C≡N) and 175 ppm (comonomer C=O). On stabilization for 60 min, two new peaks at 135 and 155 ppm were clearly observed, and in addition the C≡N became clearly unsymmetrical with a trailing low frequency wing suggesting a third new peak at ca. 115 ppm. The C=O peak at 175 ppm was apparently unchanged in chemical shift but it became somewhat more intense on stabilization, suggesting the formation of new carbonyl species related to the IR peak which appeared at 1680 cm^{-1} as discussed earlier. A high resolution ^{13}C NMR spectrum of soluble polymer extracted from SAF fibre stabilized at 225°C for 15 min did not show any peaks corresponding to those at 135 and 155 ppm in the solid state spectrum, but did have a carbonyl peak at 170 ppm.

3.5. Degree of orientation

Table 6 gives measures of orientation from WAXS and FTIR microscopy for fibres and films of DT and SAF. A significant degree of molecular orientation in fibres and stretched films is indicated by the WAXS azimuthal peak width, as well as by D_{CN} , which reflects the overall orientation of the nitrile groups in a sample, and for SAF by D_{CO} , which relates to the comonomer carbonyl. A point to note is that additional stretching of an SAF film, from 100% to 200%, did not affect D_{CN} or D_{CO} , whereas the WAXS azimuthal peak width decreased.

Fig. 8 provides a comparison of values of azimuthal peak width obtained from fibre bundles with a conventional source and from single fibres with a synchrotron source, for SAF heat-treated at 200°C. WAXS data could be obtained from bundles, but not from single fibres, for heat-treatments of more than 30 min at 225°C and at higher

Table 6
Orientation measurements for DT and SAF fibres and films

	DT WAXS peak width (deg.)	IR D_{CN}	SAF WAXS peak width (deg.)	IR D_{CN}	D_{CO}
Fibre bundle	30	—	30	—	—
Single fibre	21.5	— 0.45	21.5	— 0.37	— 0.23
Cast film	—	— 0.01	—	0.02	0.00
Film, 100% stretch	20.2	— 0.47	27.9	— 0.42	— 0.23
Film, 200% stretch	—	—	23.2	— 0.43	— 0.22

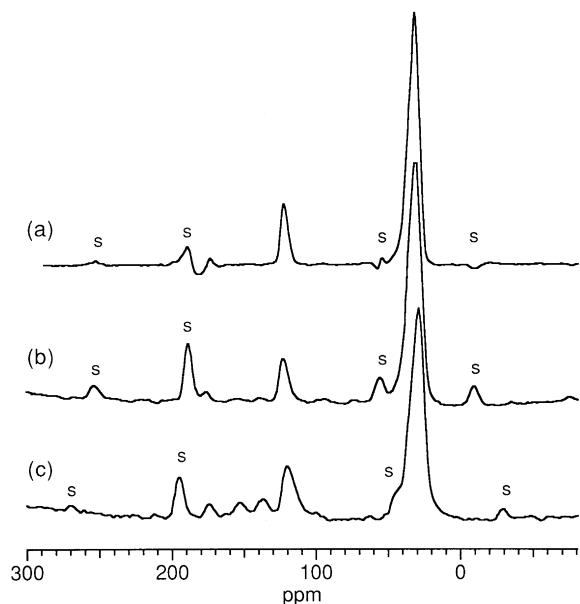


Fig. 7. Solid-state CP/MAS ^{13}C NMR spectra for (a) SAF, (b) SAF heat-treated for 15 min. at 225°C and (c) SAF heat-treated for 60 min. at 225°C . Spectrum (a) was obtained using the TOSS technique, spectra (b) and (c) are standard spectra. The label s indicates residual or actual spinning sidebands. The spin rate was ca. 5 kHz.

temperatures. Figs. 9–12 show the dependence on EOR of WAXS azimuthal peak width from fibre bundles and of D_{CN} from polarized FTIR microscopy of single fibres.

4. Discussion

4.1. Single fibre studies

A synchrotron source enabled WAXS patterns to be observed for pristine and lightly heat-treated single fibres, although there was insufficient scattering intensity from

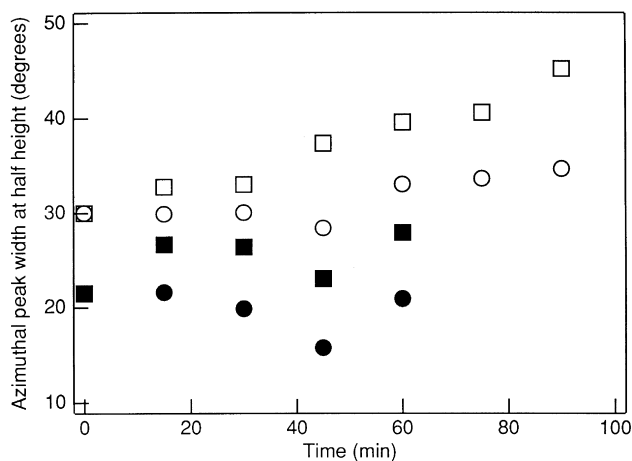


Fig. 8. Dependence on time of azimuthal peak width at half-height for SAF heat-treated at 200°C (\circ , \bullet) under tension and (\square , \blacksquare) without tension, from (open symbols) fibre bundles with a conventional X-ray source and from (filled symbols) single fibres with a synchrotron source.

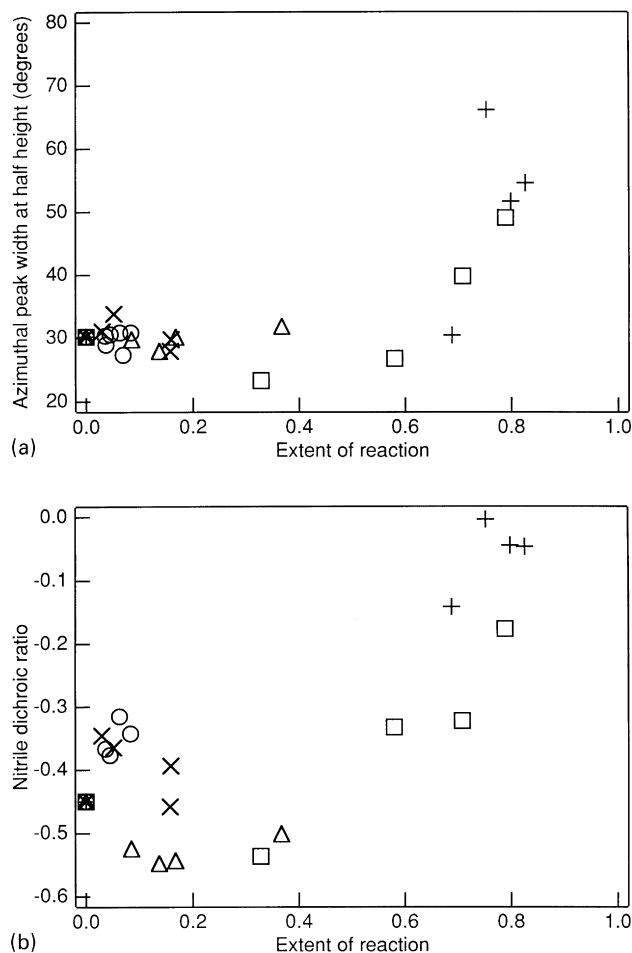


Fig. 9. Dependence on extent of reaction of (a) WAXS azimuthal peak width at half-height and (b) nitrile dichroic ratio for DT heat-treated under tension at (\circ) 200°C , (\times) 225°C , (Δ) 250°C , (\square) 275°C and ($+$) 300°C .

more heavily heat-treated single fibres. The results in Table 6 and Fig. 8 show that single fibres gave consistently lower values of azimuthal peak width than bundles, reflecting the difficulty in achieving exactly parallel alignment of all fibrils in a bundle. Single fibre data would thus be preferred for a quantitative analysis of orientation. However, carefully prepared bundle samples showed the same trends as single fibres, and were suitable for comparative studies.

Unpolarized and polarized infra-red spectra were successfully obtained from single fibres with an FTIR microscope. This enabled chemical changes to be followed, provided an internal measure of extent of reaction and gave an indication of orientation complementary to that from WAXS. It can be seen from Figs. 9–12 that values of D_{CN} for heat-treated fibres followed broadly similar trends to azimuthal peak width from WAXS.

4.2. Molecular order in PAN

Reasonable agreement with the somewhat sparse WAXS data from PAN may be claimed for a number of quite different models, ranging from Hobson and Windle's

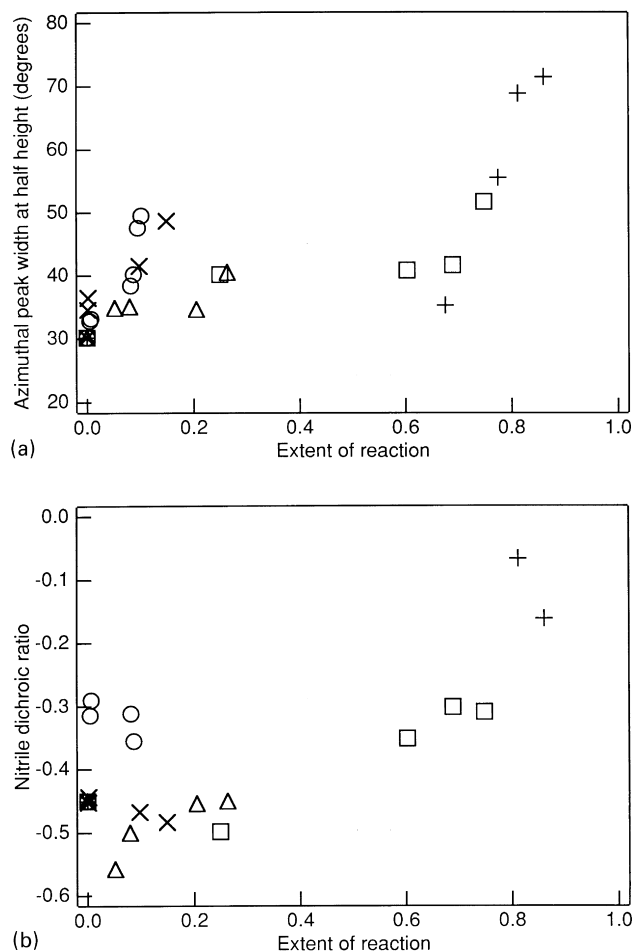


Fig. 10. Dependence on extent of reaction of (a) WAXS azimuthal peak width at half-height and (b) nitrile dichroic ratio for DT heat-treated without tension at (○) 200°C, (×) 225°C, (△) 250°C, (□) 275°C and (+) 300°C.

model of mixed tacticity crystals [50,51], to Liu and Ruland's single-phase model of kinked zig-zag chains with rotational disorder [27]. One question which has not been addressed in recent modelling studies concerns the role of intermolecular nitrile interactions. Saum [77], on the basis of an analysis of the physical properties of various organic nitriles, proposed that nitriles form dimers through dipolar interactions. He estimated the strength of a CN dipole-pair bond to be about 33 kJ mol^{-1} , greater than that for a hydrogen bond in an alcohol. There is no conclusive evidence that this type of bond occurs in PAN, but intuitively it seems likely that it does arise and that it influences the microstructure. It was a consideration of nitrile interactions which led to the concept of a "distorted helix" conformation for PAN [13,25,26].

Bashir [32] has argued that solvent-free PAN exhibits just two equatorial WAXS peaks, and that the additional WAXS peaks which have been observed are related to the presence of residual solvent. It is shown in the present study that for pristine DT, whilst conventional WAXS gave an apparently simple picture, synchrotron WAXS revealed the more

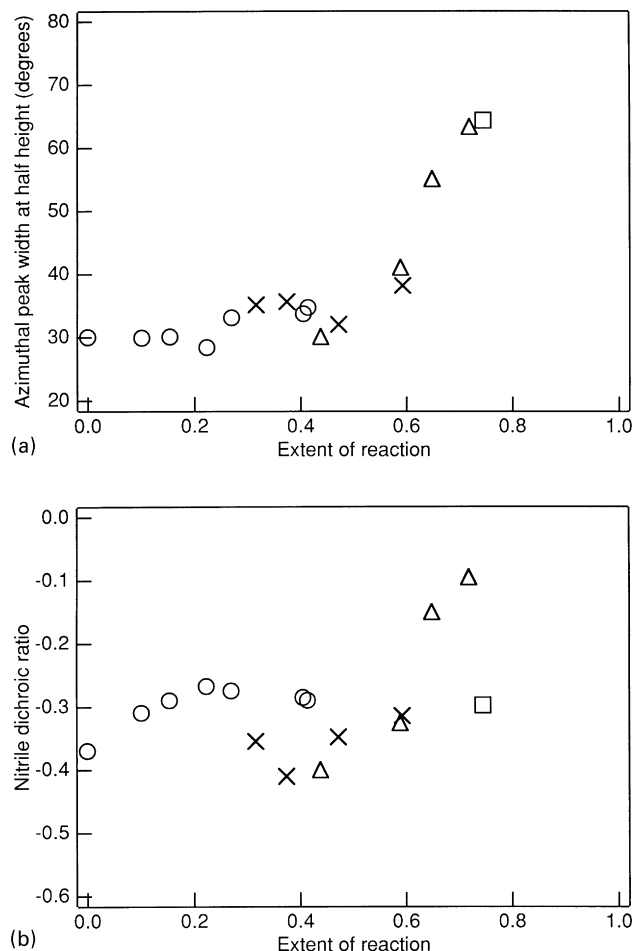


Fig. 11. Dependence on extent of reaction of (a) WAXS azimuthal peak width at half-height and (b) nitrile dichroic ratio for SAF heat-treated under tension at (○) 200°C, (×) 225°C, (△) 250°C and (□) 275°C.

complex pattern. We are inclined to the view that the additional WAXS peaks were a genuine, if minor, feature of the microstructure of the PAN, but one cannot entirely discount the possibility that the additional peaks arose as a result of traces of solvent complexed with the polymer.

The scattering at $d \approx 3.3 \text{ \AA}$, which has been ascribed to amorphous material by some workers [48,49], was observed here as an equatorial arc, indicating that the bulk of the polymer was oriented in drawn fibres. It is possible, however, that there were small regions of three-dimensional crystallinity within a less highly ordered matrix.

Synchrotron WAXS revealed a sharp meridional peak for SAF, and for DT annealed at 100°C, in addition to the diffuse meridional scattering which has been reported previously. Further, a second sharp, meridional peak arose in SAF on heat treatment at 200°C. Transitions have been observed in PAN by dynamic mechanical measurements at around 100°C and 150°C, and have been attributed to molecular motion in a paracrystalline phase and an amorphous region, respectively [78,79]. From the present observations, it seems likely that both transitions are actually related to crystalline changes.

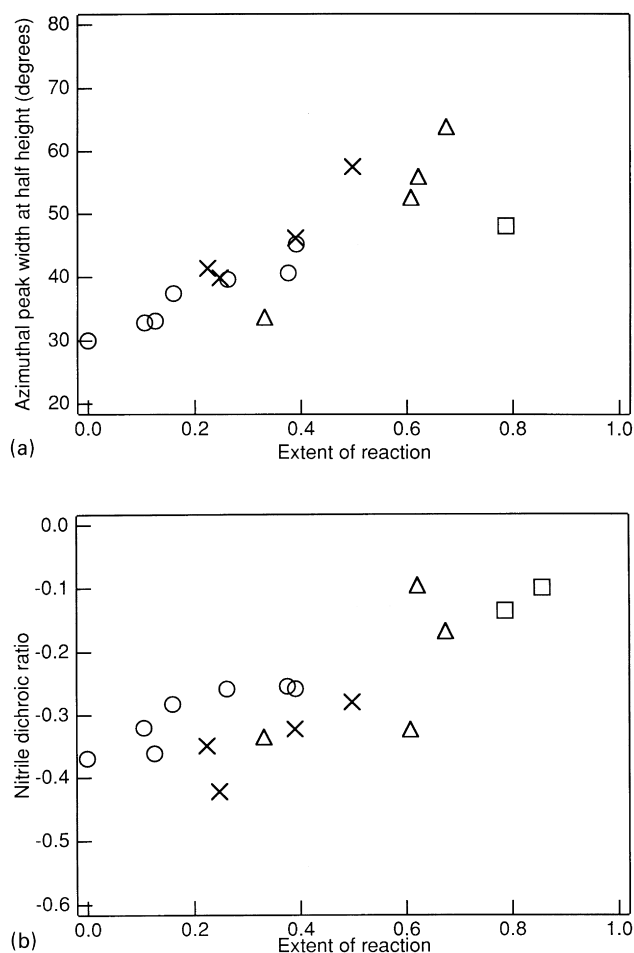


Fig. 12. Dependence on extent of reaction of (a) WAXS azimuthal peak width at half-height and (b) nitrile dichroic ratio for SAF heat-treated without tension at (○) 200°C, (×) 225°C, (Δ) 250°C and (□) 275°C.

4.3. Effect of stabilization on molecular orientation

It can be seen in Figs. 9 and 11 that, for fibres heat-treated under tension, the WAXS azimuthal peak width was constant up to EOR = 0.5, and increased thereafter (orientation decreased). If PAN could be treated as a conventional semi-crystalline polymer, this might be taken to indicate that stabilization reactions were initially limited to an amorphous phase, as suggested by Chatterjee et al. [54] However, if this were the case, one would expect a substantial change in D_{CN} over the same period, reflecting an increasing proportion of unreacted nitrile groups in the crystalline phase, and this was not observed. It is more likely that reaction of nitrile groups occurred throughout the bulk of the material. The fact that orientation was maintained to fairly high extents of reaction helps to explain the relationship between precursor properties and carbon fibre properties. For fibres allowed to relax during heat-treatment (Figs. 10 and 12) there was, not surprisingly, a generally more rapid loss of orientation.

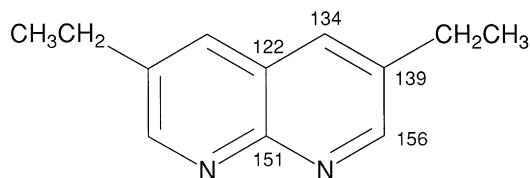


Fig. 13. ¹³C NMR chemical shift assignments for 3,6 diethyl-1, 8-naphthyridine.

4.4. Chemical changes during stabilization

The spectroscopic results suggest that at least three processes occurred in the early stages of stabilization:

1. Reaction of nitriles to give conjugated C = N containing structures. This could be intramolecular, resulting in cyclization [4–11], or intermolecular, resulting in cross-linking [12–14]. It is not possible to distinguish conclusively between these possibilities, though the observation that the dichroism of the IR peak at 1600 cm⁻¹ was opposite to that of the initial nitrile at 2240 cm⁻¹ may be considered to favour the former.
2. Generation of conjugated C = C structures. These could result from dehydrogenation [10,73], or arise from imine–enamine tautomerization and subsequent isomerization [9–11].
3. Oxidation, giving rise to a carbonyl group.

The fact that in ¹³C NMR, only peaks from unsaturated carbons developed on heat-treatment suggests that structures **b** and **c** in Table 1 can be discounted, as these would generate new types of sp³ carbons. Some support for structure **a** is provided by estimations of chemical shifts in the model structure shown in Fig. 13, calculated using experimental chemical shifts for the base heterocycle 1,8-naphthyridine from Ref. [80] together with ethyl substituent parameters for benzene from Ref. [81]. Solid state ¹³C NMR (Fig. 7) showed that conjugated C = N and C = C structures were formed in SAF after just 15 min at 225°C. Soluble polymer extracted from SAF heat-treated under these conditions did not exhibit ¹³C NMR peaks attributable to C = N or C = C, demonstrating that it is the formation of these structures which makes the polymer insoluble. Significantly, the soluble polymer exhibited a carbonyl peak at 170 ppm, which does not appear to be caused by the comonomer. This may be explained in terms of oxidation resulting in chain scission [21,22]. Chain degradation thus appears to be a competing process to the formation of conjugated structures on stabilization of PAN in air.

5. Conclusions

(1) Use of a synchrotron source allowed WAXS data to be obtained from single untreated and lightly heat-treated PAN fibres. For orientation measurements, single fibres gave consistently smaller arc widths than fibre bundles. However,

the use of fibre bundles with a conventional source was adequate for comparative studies.

(2) FTIR microscopy enabled spectra to be obtained from single fibres. The parameter $EOR = [I_{1600}/(I_{CN} + I_{1600})]$ was a useful comparative measure of extent of reaction during the early stages of the stabilization of PAN. Dichroic ratio provided a complementary measure of orientation to that from WAXS.

(3) With a synchrotron source, seven equatorial WAXS reflections could be detected in homopolymer PAN fibre bundles. Sharp meridional peaks could be observed in PAN fibres under certain conditions. In drawn PAN fibres, the bulk of the polymer was oriented. PAN may best be perceived in terms of lateral ordering of distorted rodlike molecules, with small regions of three-dimensional crystallinity.

(4) For fibres heat-treated under tension, orientation was maintained up to $EOR = 0.5$ and only then diminished; this is of significance for carbon fibre production.

(5) Three processes (nitrile reaction, conjugated C=C formation and oxidation) all occurred during the early stages of stabilization in air. The first two gave rise to insoluble polymer, but oxidation may have led to chain scission.

Acknowledgements

We are grateful to EPSRC and BP for provision of a CASE studentship for SD, to Daresbury Laboratory for provision of SRS beamtime, to the BP Research Centre, Sunbury-on-Thames, for access to a FTIR microscope, and to Colin Nave, David Gilbert and Mary Vickers for helpful discussions.

References

- [1] Sen K, Hajir Bahrami S, Bajaj P. *J Macromol Sci: Rev Macromol Chem Phys* 1996;C36:1.
- [2] Bajaj P, Roopanwal AK. *J Macromol Sci: Rev Macromol Chem Phys* 1997;C37:97.
- [3] Bashir Z. *Carbon* 1991;29:1081.
- [4] Houtz RC. *Textile Res* 1950;20:786.
- [5] Grassie N, Hay JN, McNeill IC. *J Polym Sci* 1958;31:205.
- [6] Grassie N, McGuchan R. *Eur Polym J* 1971;7:1091; 1971;7:1357; 1971;7:1503; 1972;8:257;1972;8:865.
- [7] Burlant WJ, Parsons JL. *J Polym Sci* 1956;22:249.
- [8] LaCombe EM. *J Polym Sci* 1957;24:152.
- [9] Coleman MM, Petcavich R. *J Polym Sci Polym Phys Edn* 1978;16:821.
- [10] Fochler HS, Mooney JR, Ball LE, Boyer RD, Grasselli JG. *Spectrochim Acta* 1985;41A:271.
- [11] Xue TJ, McKinney MA, Wilkie CA. *Polym Degrad Stab* 1997;58:193.
- [12] Grassie N, Hay, JN. *J Polym Sci* 1962;56:189.
- [13] Olivé GH, Olivé S. *Adv Polym Sci* 1979;32:12; 1983;51:1.
- [14] Schurz J. *J Polym Sci* 1958;28:438.
- [15] Berlin AA, Dubinskaya AM, Moshkovski Yu Sh. *Polym Sci USSR* 1966;6:2145.
- [16] Fester W. *Textil rundschau* 1965;20:1.
- [17] Peebles LH, Brandrup J. *Makromol Chem* 1966;98:189.
- [18] Standage AE, Matkowsky RD. *Eur Polym J* 1971;7:775.
- [19] Conley RT, Bieron JF. *J Appl Polym Sci* 1963;7:1757.
- [20] Frigge K, Büchtemann A, Fink H-P. *Acta Polym* 1991;42:322.
- [21] Ferguson J, Mahapatro B. *Fibre Sci Tech* 1976;9:161.
- [22] Jellinek HHG, Das A. *J Polym Sci Polym Chem Edn* 1978;16:2715.
- [23] Bahl OP, Mathur RB, Kundra KD. *Fibre Sci Tech* 1981;15:147.
- [24] Chari SS, Bahl OP, Mather RB. *Fibre Sci Tech* 1981;15:153.
- [25] Rosenbaum S. *J Appl Polym Sci* 1965;9:2071.
- [26] Hu X, Johnson DJ, Tomka JG. *J Text Inst* 1995;86:322.
- [27] Liu XD, Ruland W. *Macromolecules* 1993;26:3030.
- [28] Baker WO, Fuller CS, Pape NR. *J Amer Chem Soc* 1942;54:776.
- [29] Bohn CR, Schaefer JR, Statton WO. *J Polym Sci* 1961;55:531.
- [30] Walner LG, Riggert K. *J Polym Sci: Polym Lett Edn* 1963;1:111.
- [31] Klement JJ, Geil PH. *J Polym Sci: Part A-2* 1968;6:1381.
- [32] Bashir Z. *J Polym Sci: Part B: Polym Phys* 1994;32:1115.
- [33] Bashir Z, Church SP, Waldron D. *Polymer* 1994;35:967.
- [34] Allen RA, Ward IM, Bashir Z. *Polymer* 1994;35:2063.
- [35] Lindenmeyer PH, Hosemann R. *J Appl Phys* 1963;34:42.
- [36] Warner SB, Uhlmann DR, Peebles Jr LH. *J Mater Sci* 1979;14:1893.
- [37] Gupta AK, Chand N. *Eur Polym J* 1979;15:899.
- [38] Grobelny J, Tekely P, Turska E. *Polymer* 1981;22:1649.
- [39] Jiang H, Wu C, Zhang A, Yang P. *Comp Sci and Tech* 1987;29:33.
- [40] Jain MK, Abhiraman AS. *J Mater Sci* 1987;22:278.
- [41] Gupta AK, Singhal RP. *J Polym Sci: Polym Phys Edn* 1983;21:2243.
- [42] Ko T-H, Lin C-H, Ting H-Y. *J Appl Polym Sci* 1989;37:553.
- [43] Holland VF, Mitchell SB, Hunter WL, Lindenmeyer PH. *J Polym Sci* 1962;62:145.
- [44] Stéfani R, Chevreton M, Garnier M, Eyraud C. *C R Hebd Seances Acad Sci* 1960;251:2174.
- [45] Stéfani R, Chevreton M, Terrier J, Eyraud C. *C R Hebd Seances Acad Sci* 1959;248:2006.
- [46] Colvin BG, Storr P. *Eur Polym J* 1974;10:337.
- [47] Hinrichsen Von G, Orth H. *Kolloid z z polymere* 1971;247:844.
- [48] Hinrichsen G. *J Polym Sci Part C* 1972;38:303.
- [49] Matta VK, Mathur RB, Bahl OP, Nagpal KC. *Carbon* 1990;28:241.
- [50] Hobson RJ, Windle AH. *Polymer* 1993;34:3582.
- [51] Hobson RJ, Windle AH. *Macromolecules* 1993;26:6903.
- [52] Mathur RB, Bahl OP, Mittal J, Nagpal KC. *Carbon* 1991;29:1059.
- [53] Ko T-H, Ting H-Y, Lin C-H. *J Appl Polym Sci* 1988;35:631.
- [54] Chatterjee N, Basu S, Palit SK, Maiti MM. *J Polym Sci: part B: Polym Phys* 1995;33:1705.
- [55] Mukhopadhyay SK, Zhu Y. *Textile Res* 1995;65:25.
- [56] Pinghua W, Jie L, Zhongren Y, Rengyuan L. *Carbon* 1992;30:113.
- [57] Gupta AK, Maiti AK. *J Appl Polym Sci* 1982;27:2409.
- [58] Fink H-P, Walenta E, Frigge K, Büchtemann A, Weigel P. *Acta Polym* 1990;41:375.
- [59] Walenta E, Fink H-P. *Acta Polym* 1990;41:598.
- [60] Tyson CN. *Nature Physical Science* 1971;229:121.
- [61] Fillery ME, Goodhew PJ. *Nature Physical Science* 1971;233:118.
- [62] Bashir Z. *Acta Polym* 1996;47:125.
- [63] Warner SB, Peebles Jr LH, Uhlmann DR. *J Mater Sci* 1979;14:556.
- [64] Schmidt DL. *US NTIS, AD Rep. AD-A047293* 1978.
- [65] Messerschmidt RG, Harthcock MA, editors. *IR microspectroscopy – theory and applications*. New York: Marcel Dekker, 1988.
- [66] Bashir Z, Tipping AR, Church SP. *Polym Int* 1994;33:9.
- [67] Zbinden R. *Infrared spectroscopy of high polymers*. New York: Academic Press, 1964:213.
- [68] Mitchell R. In: Booth C, Price C, Allen G, Bevington JC, editors. *Comprehensive polymer science*. Vol. 1, ch. 31, Oxford: Pergamon, 1989.
- [69] Schaefer J. *Macromolecules* 1971;4:105.
- [70] Turska E, Grobelny J, Dworak A, Adamowicz H. *Acta Polym* 1981;32:114.
- [71] Bovey FA. *High resolution NMR of macromolecules*. New York: Academic Press, 1972.
- [72] Watt W, Johnson W. *Nature* 1975;257:210.
- [73] Usami T, Itoh T, Ohtani H, Tsuge S. *Macromolecules* 1990;23:2460.

- [74] Coleman MM, Sivy GT, Painter PC, Snyder RW, Gordon B. Carbon 1983;21:255.
- [75] Zhu Y, Wilding MA, Mukhopadhyay SK. J Mater Sci 1996;31:3831.
- [76] Dixon WT. J Chem Phys 1982;77:1800.
- [77] Saum AM. J Polym Sci 1960;42:57.
- [78] Minami S. Appl Polym Symp 1974;25:145.
- [79] Rizzo P, Guerra G, Auriemma F. Macromolecules 1996;29:1830.
- [80] van der Plas HC, Felfhuizen A, Wozniak M, Smith P. J Org Chem 1978;43:1673.
- [81] Breitmeier E, Voelter W. Carbon-13 NMR spectroscopy. High-resolution methods and applications in organic chemistry and biochemistry. Weinheim, Germany: VCH, 1987:319.